



Technical Note SC-XRD 12

New Developments in Pixel Array Technology

- Hybrid Photon Counting and Charge-Integrating Pixel Detectors

The introduction of hybrid pixel area detectors (HPAD), also known as hybrid photon-counting detectors (HPCs), has led to a great increase in the efficiency of crystallographic beamlines. These detectors offer a number of highly desirable characteristics, including high frame rates with zero dead time – allowing shutterless data acquisition and single-photon sensitivity.

Despite their advantages, however, HPADs are not perfect photon counters; not every X-ray that hits the detector is detected. At high count rates, X-rays are lost due to count rate saturation. At the pixel boundaries, X-rays are also lost due to charge-sharing noise. Finally, for higher

energy Mo $K\alpha$, and Ag $K\alpha$ radiation) the effective absorption of most HPADs is quite low, which reduces the Detective Quantum Efficiency (DQE). Due to these limitations, HPADs' effective noise can be up to hundreds of times higher than that of a perfect photon-counting detector.

These drawbacks limit the data accuracy that can be achieved with conventional HPADs. A new generation of detectors, Charge-Integrating Pixel Detectors (CPADs), has recently been introduced that preserves HPADs' desirable characteristics (e.g., fast frame rates and single-photon sensitivity) while essentially eliminating count rate saturation and charge-sharing problems.

This Technical Note examines the origins of count rate saturation, charge-sharing noise, and high-energy efficiency losses in conventional HPADs. It discusses how the new generation of CPADs avoids these sources of noise, achieving DQEs up to hundreds of times better than HPADs – very close to a perfect photon counter.

Count Rate Saturation

Perhaps the most well-known problem associated with photon-counting detectors is that they require a finite interval of time to count a single X-ray event. This interval (typically on the order of a microsecond) is due to the time required for the charge cloud to drift through the sensor, and also due to the counting electronics' bandwidth [1].

Therefore, if multiple X-rays interact with a single pixel within this microsecond time interval, all of the overlapping pulses will not be counted (Figure 1a). This effect is commonly called count rate saturation.

Count rate saturation causes count rates above about 10^5 counts per second per pixel to become nonlinear as shown in Figure 1b [2]. In principle, since the count rate loss curve is reproducible (as long as the incident count rate is constant), this effect can largely be corrected in software. However, in actual crystallographic practice, this is seldom the case since, as the sample is being rotated through its rocking curve the incident intensity is continuously changing, and thus software correction is only approximate, leaving residual errors typically on the order of a percent [2]. The effect of count rate saturation can also be reduced using time-over-threshold techniques, also called 'instant retriggering', in which – if an above-threshold output pulse continues longer than expected for a single X-ray – two overlapping events are assumed [3]. This technique extends the linear counting range up to approximately 10^7 counts per pixel per second. However, this approach also increases the read-out electronics' complexity and cost, and it is therefore often not used in detectors for laboratory applications.

At counting rates higher than about 10^7 counts per second, conventional photon-counting detectors become essentially unusable. For example, at an X-ray Free Electron Laser (XFEL) source, all the diffracted

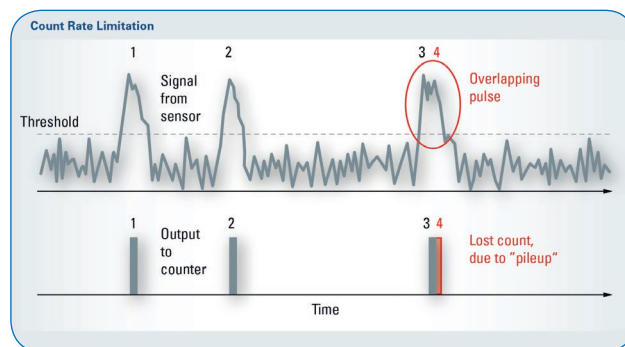


Figure 1a: Overlapping pulses are not counted in a typical HPC (hybrid photon counting pixel array) due to count rate limitation.

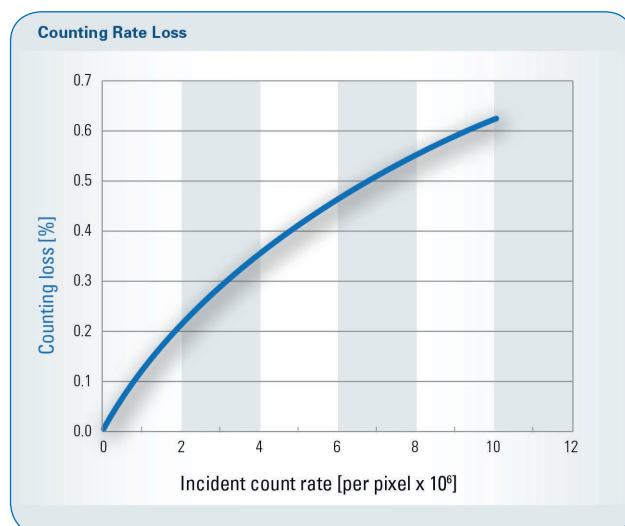


Figure 1b: Count rate loss versus incident counting rate for a typical HPC [2]. Note that 10% count rate loss typically occurs at about 10^6 counts per pixel per second.

X-rays hit the detector within a few femtoseconds. Because the incident events are essentially simultaneous, photon-counting detectors cannot be used for XFEL experiments [4].

This is one of the primary reasons that the new generation of Charge-Integrating Pixel Array Detectors (CPADs) has been developed. As described in more detail below, this type of detector has essentially no count rate limitation – a key requirement for XFEL use. However, elimination of count rate saturation is also a significant benefit for third-generation synchrotron experiments and even in a growing class of experiments in the home lab [5, 6].

Charge Sharing noise

The perhaps less well-known – but certainly more insidious – effect that leads to stochastic counting losses (which, in information theory, is equivalent to noise) in conventional HPAD detectors is charge sharing. It should be noted that HPADs, in fact, do not really count photons directly; instead, they count the clouds of charge that are produced when an X-ray is absorbed by the detector’s conversion layer material.

In all pixel-based detector designs, charge sharing occurs when an X-ray is absorbed near the boundary between adjacent pixels. In this case, the charge cloud produced by the X-ray is divided or “shared” between the adjacent pixels.

In conventional HPAD detectors, an X-ray is identified by comparing the charge cloud’s pulse height to a simple binary threshold, ideally set at half the average pulse height (assuming monochromatic X-rays). This works very well when an X-ray is absorbed in the center of a pixel (and thus all of the generated charge is confined to one pixel). However, if the X-rays are absorbed near the pixel boundaries, instead of one large pulse, two or more smaller pulses are produced in the adjacent pixels (as shown schematically in Figure 3a). These smaller pulses then fall below the binary threshold and are not counted.

This makes a part of each pixel effectively insensitive to X-rays. Note that it is not charge sharing alone that

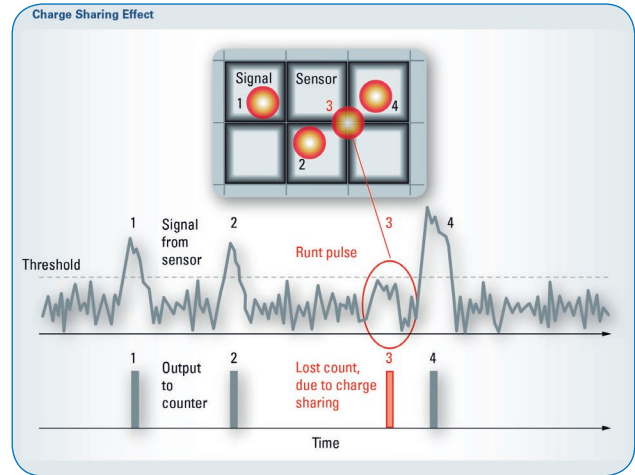


Figure 3a: Charge sharing between adjacent pixels leads to smaller pulses which are then not properly counted.

leads to counting losses; rather, it is the combination of charge sharing and simple binary thresholding. In fact, this type of information loss occurs in any image that has been subjected to binary thresholding (Figure 3b).

The combination of charge sharing and thresholding thus results in a dead area in the form of a “frame” around the boundary of each pixel. This effect has been calculated by Shanks [7] and Bergamashi [8] as shown in Figure 4. Note that this insensitive area is largest in the pixels’ corners, where the charge is divided between four adjacent pixels.

Information Loss due to Binary Thresholding

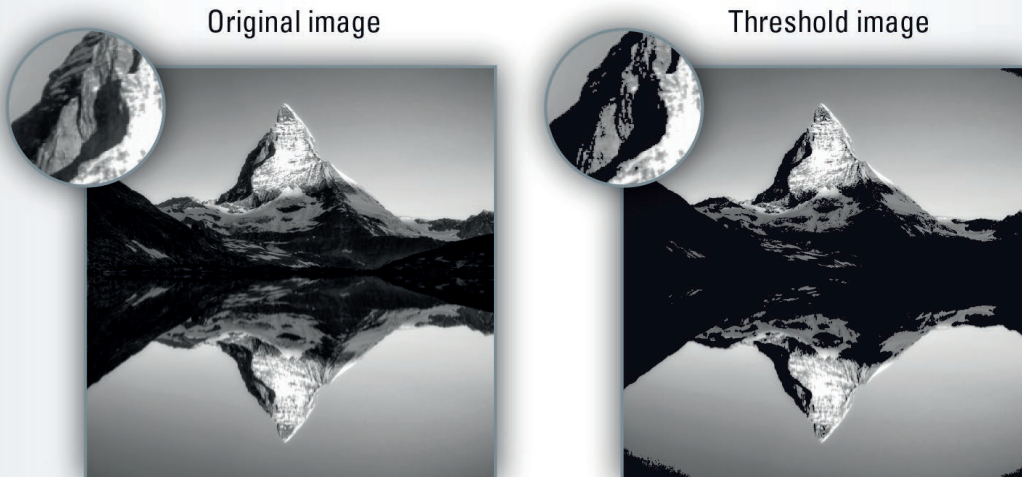


Figure 3b: Binary thresholding of an image. Applying a binary threshold to an image results in irreversible information loss. In photon-counting detectors, the charge sharing effect combined with binary thresholding leads to information loss (which, according to information theory, is equivalent to noise).

The width of the insensitive region is typically in the range of 15-20 microns (depending on the sensor's thickness and bias voltage). Because the insensitive area's width does not scale with the pixel size, the relative insensitive area becomes larger – and the problem thus becomes more serious – for smaller pixels. For example, for 100-micron pixels, approximately 35% of the pixel active area will be compromised by charge sharing. This effect was calculated by Bergamashi [8] and confirmed experimentally by Maj [9] as shown in Figure 5.

How much does this charge-sharing loss impact data quality? This depends strongly on the size of the reflections. The worst case is when the reflection size is comparable to (or smaller than) the pixel size: when the reflection falls near the corners of four adjacent pixels, it is largely undetected, whereas when it falls in the center, it is fully registered. However, if the reflection is large compared to the pixel size, the charge-sharing loss is averaged over several pixels, lessening its impact on

data quality. The magnitude of the effect can be quantified by considering the Detective Quantum Efficiency (DQE). The DQE is the ratio of the noise in an ideal detector (that is, quantum statistical noise) compared to the noise of the real detector. So, for example, a detector with a DQE of 1 would behave as an ideal detector (that is, the noise would be limited by quantum statistics only), while a detector with a DQE of 0.1 would have noise ten times higher than an ideal detector.

The impact of charge sharing on DQE was computed by Shanks using Monte Carlo techniques [7]. Figure 6 shows the DQE for a reflection with 10,000 X-rays for reflection sizes from 25 microns to 300 microns for a pixel size of 75 microns.

Note that, for reflections larger than the pixel size, the charge-sharing effect is small. However, it becomes very significant for reflections smaller than the pixel size: for 25-50 micron reflections, the effective noise is 40-100 times higher than that of an ideal detector.

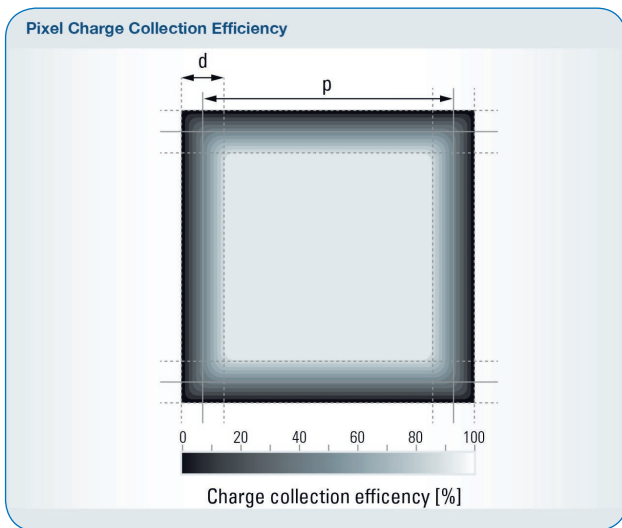


Figure 4: Charge sharing area surrounding a pixel [2]. There is a thin insensitive strip at the edge of each pixel and a larger insensitive area at each corner. Reflections that fall onto these insensitive areas will lose some X-rays.

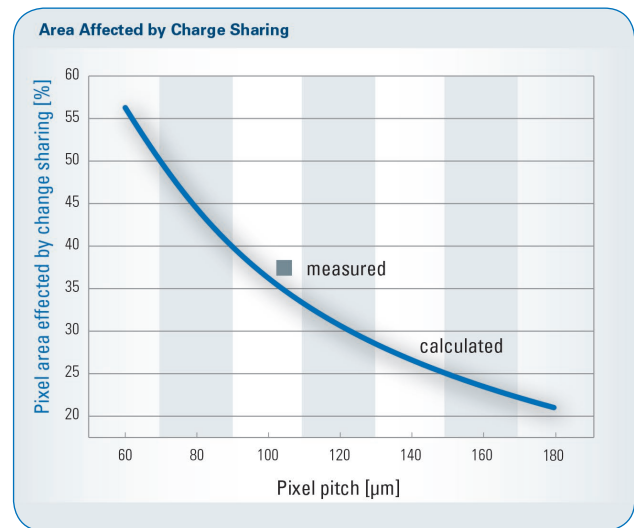


Figure 5: The percentage of the total active area which is affected by charge sharing as a function of pixel size. Smaller pixels are more strongly affected by charge sharing than larger pixels. For 170 micron pixels, only about 20% of the active area is affected by charge sharing, but for 100 micron pixels, this increases to about 40%.

What does this mean in practice for the crystallographer? A 10,000 X-ray reflection would imply an R factor of 1% for an ideal detector. For a large reflection (for example, 300 microns), a conventional HPAD will achieve an R factor very close to this value. However, for a small reflection (for example, 50 microns), the R factor will be quite drastically degraded to 10% for the same intensity.

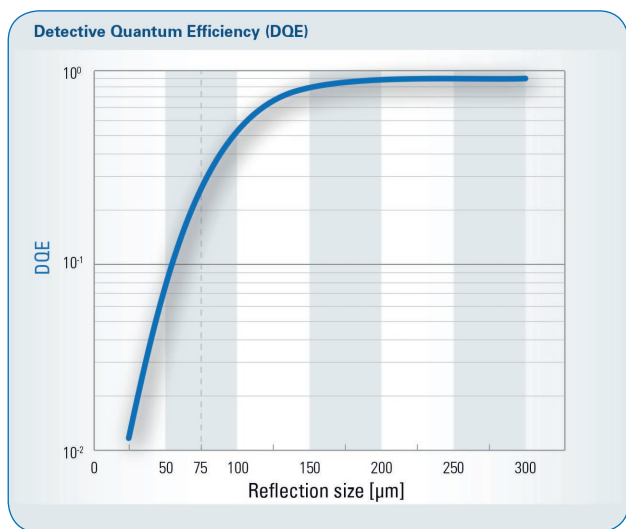


Figure 6: Detective Quantum Efficiency (DQE) for a 10,000 X-ray reflection as a function of size (for a 75 μm pixel size). For reflections larger than about twice the pixel size, the effect of charge sharing is small since the effect is then averaged out. However, it becomes increasingly significant for reflections smaller than the pixel size.

In general it is exactly such challenging, smaller samples (samples on the order of 100 μm and smaller for a 100 micron pixel) where achieving the highest possible data quality is most important and thus it is significant that HPADs struggle with these challenging samples.

It is often incorrectly claimed that HPAD detectors have no noise. It is indeed correct to say that pixel array detectors have no electronic read noise and also very little time-dependent noise (that is, no dark current noise) as is seen in, for example, CCD detectors. However, according to information theory, any loss of signal must be considered as a noise source. Therefore as Figure 6 shows, charge sharing is a very real source of noise in HPADs and, in certain situations – namely, when reflections are small – it can be very significant indeed.

Energy Range

Any detector's upper energy range is limited by absorption within the sensor. Typically, HPAD detectors employ Si as a sensor material, since it can be obtained commercially with defect densities lower than any other commercially-available material (to avoid charge recombination).

Unfortunately, however, Si is also a relatively poor absorber of high-energy X-rays (as shown in Figure 7). Si is an efficient absorber of X-rays at low energies, but its efficiency of absorption drops sharply at higher energies. For example, its absorption efficiency at Ag $\text{K}\alpha$ drops to only 50% for a 1 mm sensor.

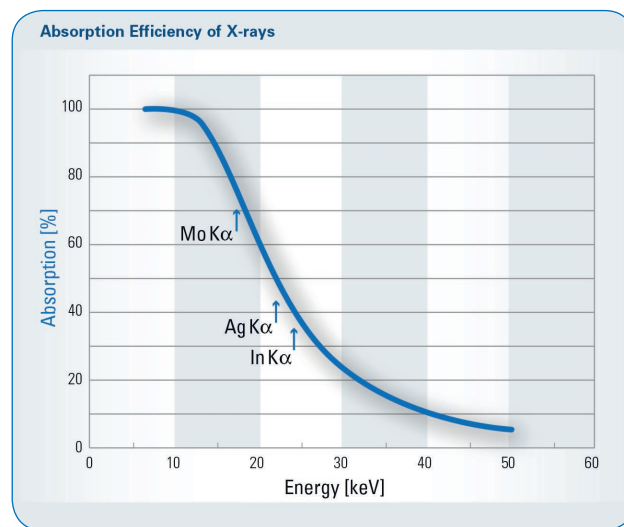


Figure 7: Absorption efficiency of X-rays versus energy in a thick Si sensor (1 mm). Note high efficiency for lower energies (below 12 keV) but strongly decreasing efficiency at higher energies including energies of common interest for laboratory diffraction such as Mo $\text{K}\alpha$ (77%), Ag $\text{K}\alpha$ (51%) and In $\text{K}\alpha$ (42%).

It is possible to increase the X-ray absorption at higher energies by employing other sensor materials, such as, for example, CdTe [10]. However, commercially-available CdTe still suffers from defect densities far higher than Si, and also has other limitations such as high costs and instabilities due to polarization. For these reasons, Si is still by far the most common sensor material for laboratory applications.

Charge-integrating Pixel Array Detectors

A new type of detector, Charge-integrating Pixel Array Detectors (CPADs), has been recently developed for applications at fourth-generation beamlines. CPADs retain the principal advantages of conventional HPAD detectors, including high frame rates and single-photon sensitivity. However, they also essentially eliminate the issues of count rate saturation and charge-sharing noise.

Though they were initially developed for use at XFELs, CPADs also offer compelling advantages – both for third-generation beamlines and for home laboratory use. Examples of this type of detector include the Jungfrau, developed for use at the SWISSFEL [11], and the CSPAD, developed for use at Stanford’s Linear Coherent Light Source [12]. In a CPAD (as in a conventional HPAD), each pixel contains its own preamplifier.

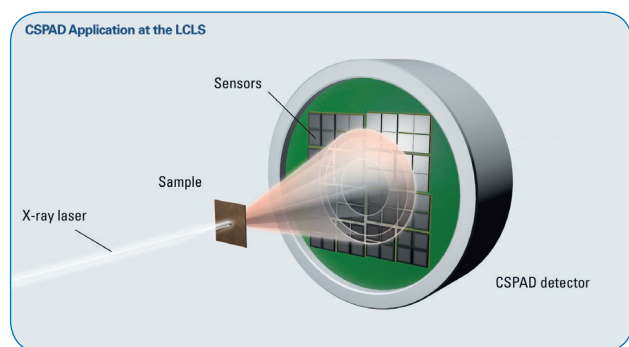


Figure 8: CSPAD detector for application at the LCLS [12].

However, in a CPAD, each X-ray pulse – in contrast to being compared with a binary threshold as in an HPAD – is stored in a local capacitor and then read out after a finite exposure time. In other words, each pixel’s total charge is integrated and then read out after the exposure. By measuring the integrated charge with very high precision, it is possible to determine each pixel’s total X-ray count with high accuracy.

CPADs can deal with extremely high count rates because there is no counting of charge pulses, meaning that there is no count rate saturation as in HPADs [4, 11].

Similarly, the lack of binary thresholding in CPADs means that there is no charge-sharing noise [11]. In contrast to HPAD detectors, in CPADs the information in the shared charge is completely preserved. The problem with conventional HPADs is not the presence of charge sharing *per se*, but the fact that the simple binary threshold throws away all of the information contained in the shared charge. In CPADs, this information is fully

retained, so charge-sharing counting noise is eliminated. Therefore, it is possible to do single photon counting without charge-sharing effects, allowing very long exposures without noise.

Because it does not suffer from count rate saturation or charge-sharing noise, a CPAD can achieve data quality close to that of an ideal detector over its entire operating range [11]. Finally, the latest CPAD designs can be used either with a semiconductor sensor (as in an HPAD) or with a scintillation converter (especially suitable for use at higher energies) [11]. This gives these detectors the flexibility to excel in a broad range of experimental situations.

Limitations of CPADs

Because the advantages of CPADs are so compelling, it is reasonable to expect that they will be adopted as the detector of choice for a wide range of applications. But do CPADs have any downsides compared to HPADs? CPADs do indeed have one significant limitation: like all integrating detectors, they suffer from full-well saturation. A CPAD can only store a finite number of X-rays per pixel, after which the full well is reached and the pixel becomes insensitive to further incident flux [4, 11, 12]. The current generation of CPADs is designed with high-frame-rate capability and high-full-well capacity to minimize this limitation [11, 12]. For example, the PHOTON II is designed to detect a sustained flux rate of up to 10^6 X-rays/pixel-sec (Cu $K\alpha$) without saturation.

The PHOTON II: the First CPAD for Home Laboratory Applications

Bruker’s PHOTON II detector is the first laboratory detector based on the latest CPAD technology. It can achieve readout rates up to 70 frames per second with zero dead time – similar to the CPADs designed for XFEL applications.

The PHOTON II thus fully supports modern shutterless data acquisition.

Also, like the XFEL designs, the PHOTON II achieves single-photon sensitivity and is thus ideal for experiments with very weakly-scattering signals.

Most crucially, like the XFEL CPADs, the PHOTON II’s freedom from count rate saturation and charge-sharing noise allows for superior data quality, especially for small samples.

Other PHOTON II features include:

- A very large active area of $140 \times 100 \text{ mm}^2$ with no gaps or insensitive areas.
- New proprietary X-ray convertor which achieves an ideal Nyquist-limited spatial resolution while achieving high DQE over a broad energy range: from 5 keV to 50 keV and above). Note that, for Ag $K\alpha$, the PHOTON II's absorption efficiency is nearly twice that of silicon-based HPAD detectors.
- A hermetically-sealed, air-cooled design eliminates the need for both cooling water and dry purging gas.
- Low weight (compared to a similarly-sized PAD detector) allows for installation on a 2theta arm for high-resolution data collection. This is particularly important for data sets using long wavelengths.

Summary

The development of 4th generation X-ray sources has necessitated the development of a new generation of CPAD detectors with significantly enhanced count rate capability and lower noise. The Bruker PHOTON II now offers this advanced CPAD technology for home laboratory use.



Figure 9: PHOTON II detector.

Literature

- [1] L. Rossi, Pixel Detectors: From Fundamentals to Applications, Springer, 2006.
- [2] P. Kraft et al., J. Synchrotron Radiation 2009 May 1; 16 (Pt 3), 368–375.
- [3] T. Loeliger et al., IEEE Nuclear Science Symposium and Medical Imaging Conference (NSS/MIC), 2012 , 610-615.
- [4] A. Koch et al., J. Physics; Conf. Ser. 425, 2013, 1-4.
- [5] C. Blome, et al., J. Phys. IV, 11, 2001, 491-492.
- [6] G. Harding, Radiation Physics and Chemistry, 67(1), 2003, 7–14.
- [7] K. Shanks, Development of Low-Noise Direct-Conversion X-ray Area Detectors for Protein Micro-crystallography, http://bigbro.biophys.cornell.edu/publications/f32_Shanks,%20Kate%20PhD%20Thesis%20sml.pdf, 2014.
- [8] J. Bergamaschi et al., J. Inst, 16th International Workshop on Radiation Imaging Detectors, 2014, 22-26.
- [9] Maj, P. et al. JINST 10, 2015, C02006.
- [10] T. Hirono et al., Nuc. Inst. and Meth. In Phys. Res. A, 11 December 2013, 64–67.
- [11] A Mozzanica et al, JINST 9, 2014, C05010.
- [12] P. Hart et al., The Cornell-SLAC Pixel Array Detector at LCLS, SLAC-PUB-15284, 2012.



 **Bruker AXS GmbH**

Karlsruhe · Germany
Phone +49 721 50997-0
Fax +49 721 50997-5654
info.baxs@bruker.com

www.bruker.com